European Journal of Immunology

Midline 1 directs lytic granule exocytosis and cytotoxicity of mouse killer T cells

Lasse Boding[1], Ann K. Hansen[1], Germana Meroni[2], Bo B. Johansen[3], Thomas H. Braunstein[4], Charlotte M. Bonefeld[1], Martin Kongsbak[1], Benjamin A. H. Jensen[1], Anders Woetmann[1], Allan R. Thomsen[1], Niels Ødum[1], Marina R. von Essen[1] and Carsten Geisler[1]

[1] Department of International Health, Immunology and Microbiology, University of Copenhagen, Copenhagen, Denmark
[2] Institute for Maternal and Child Health - IRCCS "Burlo Garofolo", Trieste, Italy
[3] Core Facility for Integrated Microscopy, University of Copenhagen, Copenhagen, Denmark
[4] Department of Biomedical Sciences, Danish National Research Foundation Centre for Cardiac Arrhythmia, University of Copenhagen, Copenhagen, Denmark

Midline 1 (MID1) is a microtubule-associated ubiquitin ligase that regulates protein phosphatase 2A activity. Loss-of-function mutations in MID1 lead to the X-linked Opitz G/BBB syndrome characterized by defective midline development during embryogenesis. Here, we show that MID1 is strongly upregulated in murine cytotoxic lymphocytes (CTLs), and that it controls TCR signaling, centrosome trafficking, and exocytosis of lytic granules. In accordance, we find that the killing capacity of MID1$^{-/-}$ CTLs is impaired. Transfection of MID1 into MID1$^{-/-}$ CTLs completely rescued lytic granule exocytosis, and vice versa, knockdown of MID1 inhibited exocytosis of lytic granules in WT CTLs, cementing a central role for MID1 in the regulation of granule exocytosis. Thus, MID1 orchestrates multiple events in CTL responses, adding a novel level of regulation to CTL activation and cytotoxicity.

Keywords: Cytotoxicity · Granule exocytosis · Midline 1 · T cells

Additional supporting information may be found in the online version of this article at the publisher's web-site

Introduction

Cytotoxic lymphocytes (CTLs) play a key role in the defense against infections. The CTL recognizes specific antigen/MHC complexes on infected target cells by the TCR. Specific recognition of a target cell leads to establishment of a stable conjugation, the immunological synapse (IS), between the CTL and the target cell [1–3]. Immediately after recognition of the target cell, the CTL polarizes its secretory machinery toward the IS. The centrosome, which in CTLs is often called the microtubule-organizing center (MTOC), relocates to the IS [4, 5], and lytic granules that contain perforin and granzymes move along the microtubules toward the MTOC [6]. Here, they dock at the plasma membrane and deliver their content by exocytosis into the small secretory cleft of the IS [3, 7, 8]. Perforin and granzymes subsequently act in concert to induce apoptosis of the target cell [9]. Thus, the microtubule cytoskeleton plays a key role in directional secretion of lytic granules and thereby in CTL-mediated target cell killing [8]. It is still not clear how CTLs regulate reorganization of the microtubule cytoskeleton and exocytosis of lytic granules during encounter with target cells.

Correspondence: Dr. Carsten Geisler
e-mail: cge@sund.ku.dk

Midline 1 (MID1) is a ubiquitin ligase that belongs to the RBCC/TRIM family, which contains a RING domain followed by B-boxes and a coiled-coil domain [10, 11]. MID1 is associated with the microtubules [12, 13] and regulates the level of microtubule-associated protein phosphatase 2A (PP2A) [14, 15]. The X-linked Opitz G/BBB syndrome (OS) is caused by mutations of *MID1* and is characterized by disorders that primarily affect the ventral midline [16]. Manifestations include ocular hypertelorism, genitourinary defects, clefts of palate and lip, trachea-esophageal fistulas, imperforate anus, and mental retardation. An accumulation of the catalytic subunit of PP2A (PP2Ac) is found in fibroblasts from patients with OS due to impairment of the ubiquitin ligase activity of the mutated MID1. The increased level of PP2Ac is associated with reduced phosphorylation of microtubule-associated proteins that regulate microtubule dynamics [14]. From these observations, it has been suggested that MID1 plays crucial roles during embryogenesis by regulating microtubule dynamics [10, 17].

Whether MID1 plays any role after embryogenesis has remained unknown until very recently, when it was found that MID1 is involved in induction of allergic airway inflammation in the bronchial epithelium [18]. Whether MID1 is expressed in T cells is unknown. As microtubule dynamics play key roles in CTL polarization and target cell killing, and as MID1 has been suggested to control microtubule dynamics during embryogenesis, we asked the question of whether MID1 is expressed in T cells and what function it might play in CTLs. We purified naïve and activated T cells and found that MID1 is indeed expressed in T cells and that it is highly upregulated in CTLs. To determine the biological function of MID1 in CTLs, we studied lymphocytic choriomeningitis virus (LCMV) specific T cells from P14 TCR transgenic mice and P14 mice crossed to MID1$^{-/-}$ mice (P14MID1$^{-/-}$ mice). We found that whereas the level of PP2Ac rapidly declined in P14 CTL following activation, it was unaffected by activation in P14MID1$^{-/-}$ CTLs. In parallel, we found affected TCR signaling and impaired polarization of the MTOC during activation of P14MID1$^{-/-}$ CTLs with concomitant reduced exocytosis of lytic granules and cytotoxicity. Transfection of MID1 into P14MID1$^{-/-}$ CTLs completely rescued lytic granule exocytosis and, in accordance, knockdown of MID1 inhibited exocytosis of the lytic granules in P14 CTLs.

Results

CD8$^+$ T cells upregulate *MID1* expression in response to TCR stimulation

During embryogenesis, *MID1* is widely expressed, whereas in adult tissues it is mainly found in the brain, heart, kidney, lung, and placenta and only weakly expressed in thymus and spleen [16, 19–21]. It is not known whether *MID1* is expressed in T cells. To address this question, we determined *MID1* mRNA expression in T cells during their development and differentiation by purification of thymocytes from C57BL/6 mice and naïve CD4$^+$ and CD8$^+$ T cells from TCR transgenic SMARTA and P14 mice, respectively. Activated CD4$^+$ and CD8$^+$ (hereafter termed CTLs) T cells were generated by stimulation of CD4$^+$ and CD8$^+$ T cells with LCMV glycoprotein $gp_{61–80}$ and $gp_{33–41}$, respectively. *MID1* mRNA expression was low in thymocytes and naïve CD4$^+$ and CD8$^+$ T cells. Activation of CD4$^+$ T cells did not significantly affect *MID1* mRNA expression. In contrast, *MID1* mRNA expression was strongly upregulated in CTLs (Fig. 1A). To study the kinetics of activation-induced *MID1* upregulation in CD8$^+$ T cells, we stimulated CD8$^+$ T cells from P14 mice for 3 days, rested them for 2 days and finally restimulated them for 1 or 2 h. At each time point, we purified the CD8$^+$ T-cell population, measured the *MID1* mRNA expression, and calculated the fold change of *MID1* expression relative to *MID1* expression in naïve CD8$^+$ T cells. We found that *MID1* mRNA expression increased seven- to eightfold during the first days of activation (Fig. 1B). During the rest period, *MID1* mRNA expression slightly declined; however, *MID1* expression rapidly increased following restimulation of the CTLs. Taken together, these results show that *MID1* is weakly expressed in naïve T cells, and that it becomes strongly upregulated in CTLs.

MID1 does not affect T-cell development and CTL expansion

To determine the biological function of MID1 in CTLs, we studied LCMV-specific T cells from P14 TCR transgenic mice and P14 mice crossed to MID1 KO mice (P14MID1$^{-/-}$ mice). First, we compared the distribution of lymphocytes in thymus, spleen, and LNs from P14 and P14MID1$^{-/-}$ mice. We found that the distribution of CD4$^+$ and CD8$^+$ T cells and CD19$^+$ B cells was unaffected in all organs tested in P14MID1$^{-/-}$ mice (Supporting Information Fig. 1). Furthermore, the total number of thymocytes was unaffected in P14MID1$^{-/-}$ mice. These results show that MID1 does not affect T-cell development.

To analyze whether MID1 affects activation, expansion, and differentiation of CD8$^+$ T cells, we stimulated splenocytes from P14 and P14MID1$^{-/-}$ mice with $gp_{33–41}$ from 0 to 6 days. We did not find any differences in proliferation or expansion of T cells

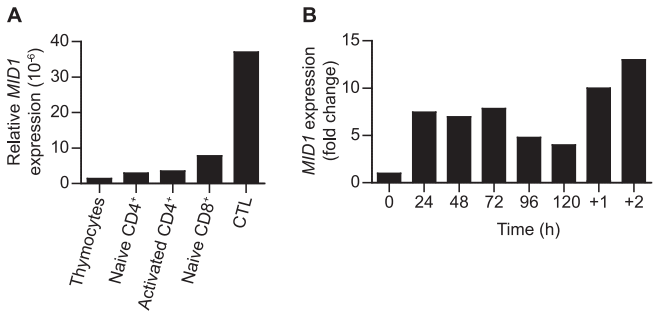

Figure 1. *MID1* mRNA expression in T cells. (A) Quantitative PCR analysis of *MID1* is shown for murine thymocytes, naïve CD4$^+$ and CD8$^+$ T cells, and activated CD4$^+$ T cells and CTLs. (B) CD8$^+$ T cells were stimulated for 0–72 h, rested for 2 days (96 and 120 h) and restimulated for 1 and 2 h (+1 and +2). The mRNA levels of *MID1* were normalized to (A) β-*actin* or to (B) *MID1* in naïve CD8$^+$ T cells. Data are shown as mean of three replicates from a single experiment representative of five independent experiments.

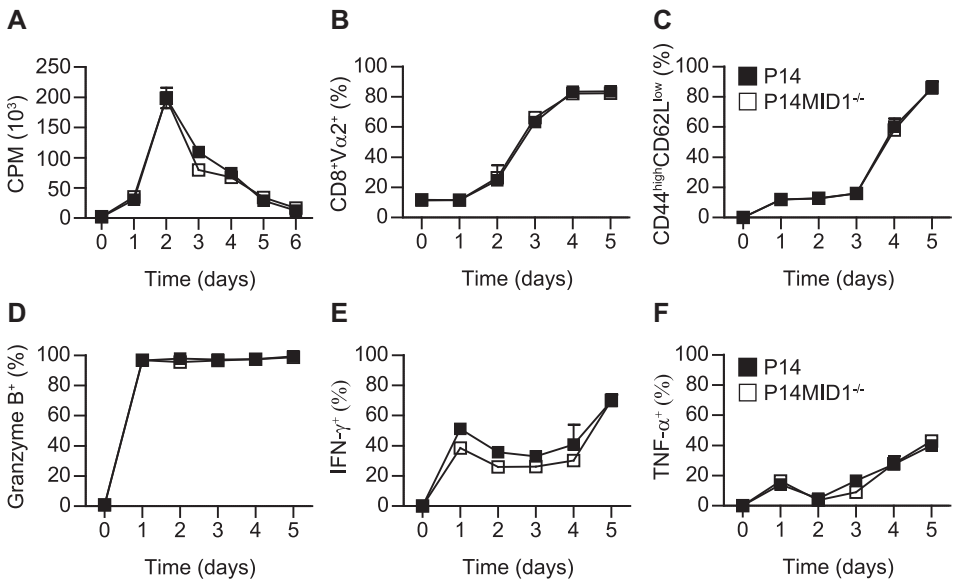

Figure 2. MID1 is not required for CTL expansion and differentiation. (A) Proliferation of P14 (black squares) and P14MID1$^{-/-}$ (white squares) CTLs as measured by ^{3}H-thymidine incorporation. The data are shown as mean ± SEM of six samples pooled from two independent experiments. (B) Expansion of P14 and P14MID1$^{-/-}$ CTLs as measured by the fraction of CD8^{+}Vα2^{+} cells in the cell cultures by flow cytometry. (C) CTL differentiation as measured by the fraction of CD44^{high}CD62L^{low}, (D) granzyme B^{+}, (E) IFN-γ^{+}, and (F) TNF-α^{+} of the CD8^{+}Vα2^{+} cells by flow cytometry. (B–F) The data are shown as mean ± SEM of three to six mice pooled from three independent experiments. For FACS gating strategy, please see Supporting Information Figure 1.

from P14 and P14MID1$^{-/-}$ mice as measured by ^{3}H-thymidine incorporation or fraction of CD8^{+}Vα2^{+} transgenic CD8^{+} T cells in the cell cultures (Fig. 2A and B). Likewise, the P14 and P14MID1$^{-/-}$ transgenic CD8^{+} T cells differentiated into CTLs with similar kinetics as determined by upregulation of CD44, downregulation of CD62L, and expression of granzyme B, perforin, IFN-γ, and TNF-α (Fig. 2C–F and Supporting Information Fig. 2). These results demonstrate that MID1 does not play a significant role in activation of naïve CD8^{+} T cells and their subsequent differentiation into CTLs.

MID1 controls TCR signaling and MTOC polarization in CTLs

A marked accumulation of PP2Ac is found in fibroblasts from patients with OS due to an impairment of the ubiquitin ligase activity of the mutated MID1 that normally targets PP2Ac for degradation [14]. To examine whether MID1 regulates the level of PP2Ac in CTLs, we restimulated P14 and P14MID1$^{-/-}$ CTLs for 0–6 h and subsequently determined the level of PP2Ac in the cells. We did not find any difference in the levels of PP2Ac in resting P14 and P14MID1$^{-/-}$ CTLs (Fig. 3A). However, following stimulation, a vigorous downregulation of PP2Ac was seen in P14 CTLs, whereas the level of PP2Ac was unaffected by stimulation in P14MID1$^{-/-}$ CTLs (Fig. 3A and B). These results show that MID1 regulates PP2Ac levels during activation of CTLs.

PP2A belongs to the family of serine/threonine phosphatases that regulates a large variety of cellular processes [22, 23], and PP2A activity is involved in the control of several signaling pathways including the mitogen-activated protein kinase pathway [24], a key pathway in TCR-induced signaling [25]. To examine whether MID1 affects TCR signaling in CTL, we measured phosphorylation of ZAP70, ERK1/2, and S6K1 (ribosomal S6 protein kinase 1) in P14 and P14MID1$^{-/-}$ CTLs stimulated for 0–2 h. Proximal TCR signaling as determined by phosphorylation of ZAP70 was unaffected in P14MID1$^{-/-}$ CTLs. In contrast, more distal TCR signaling as determined by ERK1/2 and S6K1 phosphorylation was significantly impaired in P14MID1$^{-/-}$ CTLs (Fig. 3C and D).

Polarization of the MTOC to the IS is required for directional secretion of lytic granules and target cell killing [26]. MTOC polarization is initiated within minutes of TCR stimulation and is regulated by a number of signaling molecules including ERK1/2 [8]. To examine whether MID1 affected MTOC polarization, we incubated live P14 and P14MID1$^{-/-}$ CTLs on coverslips coated with anti-CD3 antibodies at 37°C for 20 min and subsequently determined the position of the MTOC relative to the surface of the coverslips by spinning disc microscopy (Fig. 3E). We found that MTOC polarization toward the anti-CD3-coated surface was significantly impaired in P14MID1$^{-/-}$ CTLs compared to P14 CTLs ($p = 0.0011$) (Fig. 3F and Supporting Information Fig. 3). To substantiate that MID1 regulates MTOC polarization, we then studied MTOC polarization following shRNA-mediated knockdown of MID1. P14 CTLs were transfected with shMID1-GFP plasmids, sorted into a shMID1-GFP^{+} and a shMID1-GFP^{-} subpopulation, and incubated on anti-CD3-coated coverslips. The MTOC position was determined by spinning disc microscopy as described above. MTOC polarization was significantly reduced in the shMID1-GFP^{-} P14 CTLs transfectants compared with the shMID1-GFP^{+} P14 CTLs transfectants (Fig. 3G). Finally, by transfecting MID1-GFP into P14MID1$^{-/-}$ CTLs, MTOC polarization was rescued (Fig. 3H), whereas transfection of P14 CTLs with MID1-GFP did not affect MTOC polarization (data not shown). Taken together, these results show that MID1 regulates distal TCR signaling and MTOC polarization in CTLs.

MID1 regulates CTL cytotoxicity and granzyme B exocytosis

Efficient CTL-mediated target cell killing depends on polarization of the MTOC to the IS and subsequent trafficking of the lytic

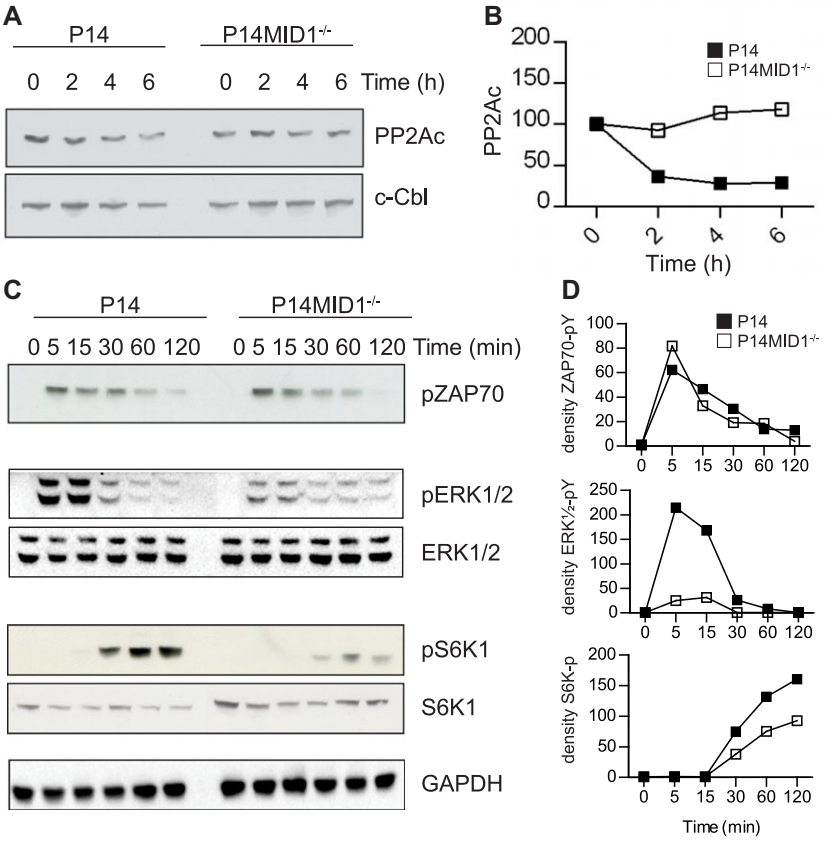

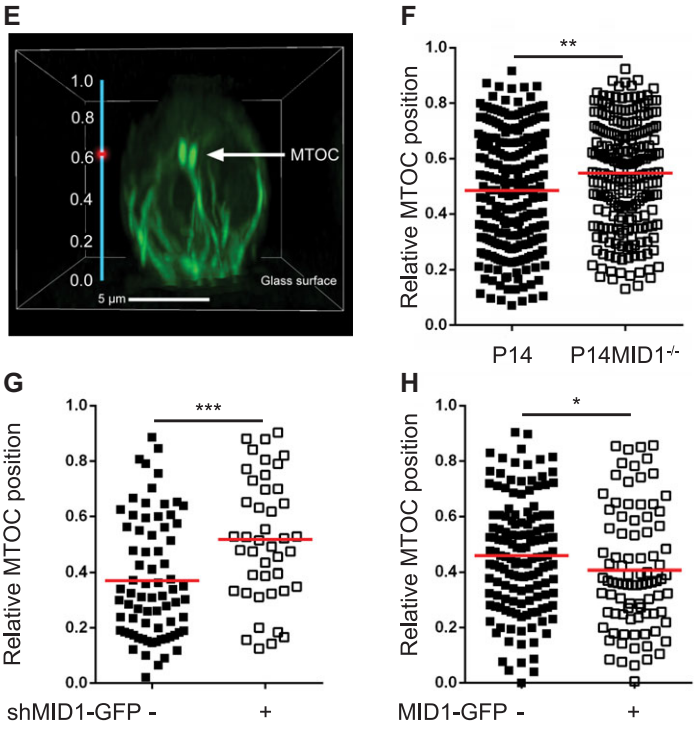

Figure 3. MID1 controls TCR signaling and MTOC polarization. (A, B) P14 and P14MID1$^{-/-}$ CTLs were stimulated with gp_{33-41} for the time indicated and PP2Ac levels were determined by Western blot. (C, D) P14 and P14MID1$^{-/-}$ CTLs were stimulated with gp_{33-41} for the time indicated and the levels of pZAP70, pERK1/2, and pS6K1 were determined by Western blot. (A, C) Data shown are representative of four independent experiments; (B, D) semiquantification for these experiments are shown. (E) Localization of the MTOC relative to the anti-CD3-coated coverslip was performed by spinning disc microscopy. Shown is a side view of a representative CTL from four independent experiments stained with Tubulin Tracker. The position of the MTOC (arrow) is indicated with a red dot at the ordinate that gives the relative MTOC position. Scale bar is 5 µm. (F) The relative MTOC position and mean value for P14 ($n = 253$) and P14MID1$^{-/-}$ ($n = 231$) CTLs from four independent experiments are shown. (G) Relative MTOC position and mean value for shMID1-GFP^{-} ($n = 74$) and shMID1-GFP^{+} ($n = 43$) P14 CTL transfectants from two independent experiments. (H) Relative MTOC position and mean values for MID1-GFP^{-} ($n = 148$) and MID1-GFP^{+} ($n = 72$) P14MID1$^{-/-}$ CTL transfectants from two independent experiments. (F–G) $^{*}p < 0.05$; $^{**}p < 0.01$; and $^{***}p < 0.001$, Mann–Whitney test.

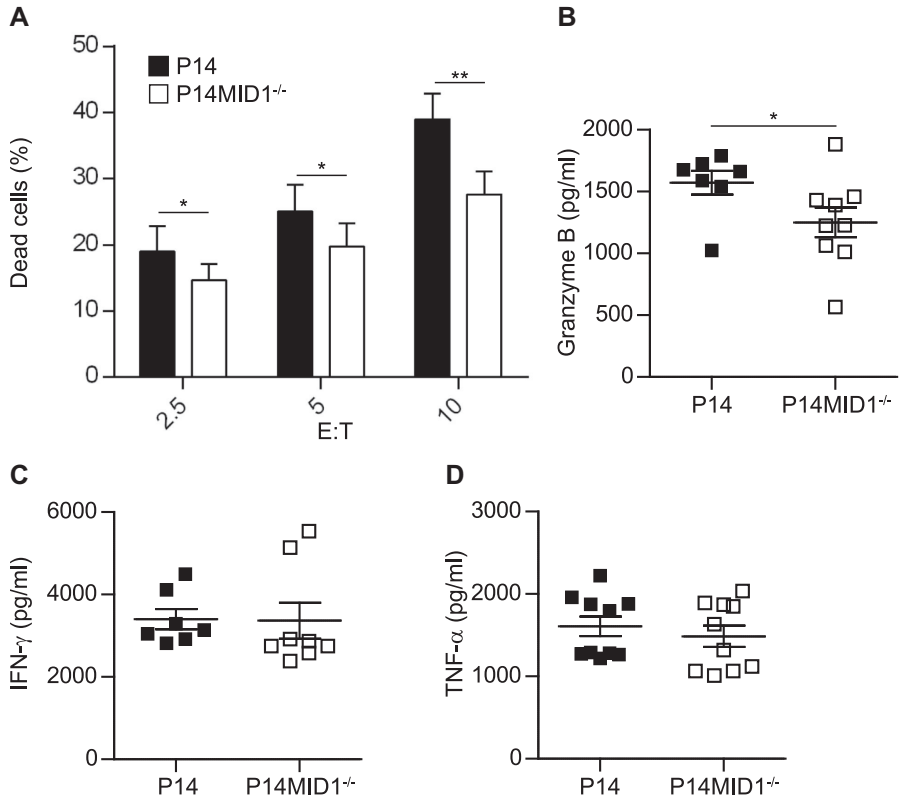

Figure 4. MID1 regulates CTL cytotoxicity and granzyme B exocytosis. (A) The fraction of dead target cells co-cultured with P14 (black squares) or P14MID1$^{-/-}$ (white squares) CTLs at the indicated effector:target (E:T) cell ratios was determined by flow cytometry. The data are shown as mean + SEM of four to six samples pooled from four independent experiments. (B–D) The concentrations of (B) granzyme B, (C) IFN-γ, and (D) TNF-α in the supernatants of P14 or P14MID1$^{-/-}$ CTLs co-cultured with peptide-pulsed splenocytes for 4 h was determined by ELISA. (B–D) The data are shown as mean ± SEM of three to ten mice pooled from three to five independent experiments. Each square represents data from one individual mouse. $^{*}p < 0.05$, $^{**}p < 0.01$, Student's *t*-test.

granules along the microtubules to the IS [7, 8, 27]. In accordance, agents that depolymerize microtubules inhibit exocytosis of lytic granules and target cell killing [5, 28]. To examine whether MID1 affects CTL-mediated cytotoxicity, we incubated P14 and P14MID1$^{-/-}$ CTLs with $gp_{33–41}$ pulsed EL-4 target cells. Since P14 and P14MID1$^{-/-}$ CTLs differentiated with identical kinetics and expressed equivalent levels of granzyme B, perforin, IFN-γ, and TNF-α (Supporting Information Fig. 2), we could directly compare these cell populations in cytotoxicity assays. CTLs and the target cells were spun together in round-bottomed plates to avoid any influence of cell migration on CTL-target cell conjugation. By using this procedure, equal numbers of P14 and P14MID1$^{-/-}$ CTL-target cell conjugates were formed (Supporting Information Fig. 4). The cytotoxicity assay revealed that the cytotoxic capacity of P14MID1$^{-/-}$ CTLs was reduced by approximately 30% compared with P14 CTLs (Fig. 4A). Next, we investigated whether the reduced target cell killing by P14MID1$^{-/-}$ CTLs could be attributed to different kinetics in the cytotoxicity of P14 and P14MID1$^{-/-}$ CTLs. However, this was not the case. The vast majority of target cell killing took place between 1 and 2 h of incubation and did not significantly increase for P14 or P14MID1$^{-/-}$ CTLs by extending the culture period to 4 h (Supporting Information Fig. 5).

To identify the cytotoxic pathway responsible for the impaired cytotoxicity, we then studied exocytosis of the lytic granules. The reduced ability to kill target cells via lytic granules could be due to diminished expression of perforin/granzyme, impaired exocytosis of the lytic granules, or a combination of the two. As we did not observe any differences in the expression levels of granzyme B and perforin in P14 and P14MID1$^{-/-}$ CTLs (Supporting Information Fig. 2), we determined exocytosis of lytic granules as measured by granzyme B secretion. We cultured P14 and P14MID1$^{-/-}$ CTLs with $gp_{33–41}$ pulsed splenocytes for 4 h and subsequently measured the concentration of granzyme B in the supernatants. P14MID1$^{-/-}$ CTLs secreted approximately 25% less granzyme B than P14 CTLs (Fig. 4B). To assess whether other secretory pathways were affected by MID1, we measured IFN-γ and TNF-α in the same supernatants. In contrast to granzyme B secretion, P14 and P14MID1$^{-/-}$ CTLs secreted equivalent amounts of IFN-γ and TNF-α (Fig. 4C and D). It has been proposed that upregulation of CD107a (LAMP1) on CTL correlates with exocytosis of lytic granule and cytotoxicity [29]. We therefore stimulated P14 and P14MID1$^{-/-}$ CTLs for 60–240 min in the presence of anti-CD107a antibodies and subsequently determined CD107a upregulation by FACS analysis. In agreement with the reduced granzyme B secretion, we found a reduced upregulation of CD107a in P14MID1$^{-/-}$ CTLs compared to P14 CTLs (Supporting Information Fig. 5G). Taken together, these results show that MID1 controls CTL-mediated cytotoxicity most likely by regulating exocytosis of the lytic granules.

MID1 controls exocytosis of lytic granules

If MID1 controls exocytosis of lytic granules, re-expression of MID1 into P14MID1$^{-/-}$ CTLs should rescue the exocytosis defect

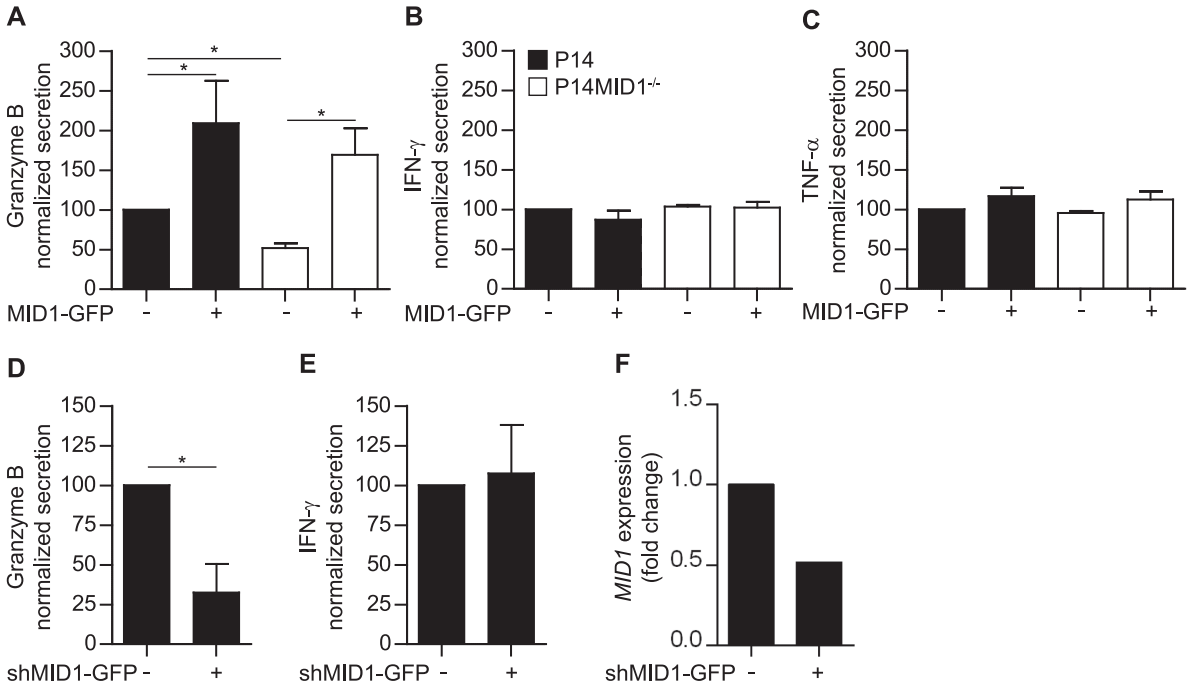

Figure 5. MID1 controls exocytosis of lytic granules. (A–C) The concentration of (A) granzyme B, (B) IFN-γ, and (C) TNF-α in the supernatants of MID1-GFP$^-$ and MID1-GFP$^+$ P14 or P14MID1$^{-/-}$ CTL transfectants co-cultured with peptide-pulsed splenocytes for 4 h was determined by ELISA. The values were normalized to secretion by the MID1-GFP$^-$ P14 CTL transfectants. (A–C) Data are shown as mean + SEM of three to ten mice pooled from three to five independent experiments. (D–E) The concentration of (D) granzyme B and (E) IFN-γ in the supernatants of shMID1-GFP$^-$ and shMID1-GFP$^+$ P14 CTL transfectants co-cultured with peptide-pulsed splenocytes for 4 h was determined by ELISA. The values were normalized to secretion by the shMID1-GFP$^-$ P14 CTL transfectants. Data are shown as mean + SEM of three samples pooled from three independent experiments. (F) Quantitative PCR analysis of *MID1* in shMID1-GFP$^-$ and shMID1-GFP$^+$ P14 CTL transfectants. The mRNA levels of *MID1* were normalized to *MID1* in shMID1-GFP$^-$ P14 CTL transfectants. The data are shown as mean of three replicas and are from a single experiment representative of two independent experiments. $*p < 0.05$, Student's *t*-test.

of P14MID1$^{-/-}$ CTLs. Consequently, we transfected P14 and P14MID1$^{-/-}$CTLs with a MID1-GFP plasmid. The transfected cells were sorted in an MID1-GFP$^+$ and an MID1-GFP$^-$ subpopulation and then stimulated for 4 h with $gp_{33–41}$ pulsed splenocytes. The supernatants were harvested and the concentration of secreted granzyme B, IFN-γ, and TNF-α determined. Transfection of MID1 into P14MID1$^{-/-}$ CTLs completely rescued granzyme B exocytosis and even increased it almost twofold compared with granzyme B exocytosis by MID1-GFP$^-$ P14 CTLs (Fig. 5A). Likewise, transfected MID1 also significantly increased granzyme B exocytosis in P14 CTLs. In contrast, neither IFN-γ nor TNF-α secretion was affected by MID1 transfection (Fig. 5B and C). To exclude that GFP in itself affected granzyme B exocytosis we transfected P14 CTLs with a control-GFP plasmid, sorted the transfected cells in a control-GFP$^+$ and a control-GFP$^-$ subpopulation and stimulated them for 4 h with $gp_{33–41}$ pulsed splenocytes and measured granzyme B in the supernatants. We found that GFP expression did not affect granzyme B exocytosis (Supporting Information Fig. 6).

To substantiate that MID1 controls exocytosis of lytic granules, we studied granule exocytosis following shRNA-mediated knockdown of MID1. P14 CTLs were transfected with shMID1-GFP plasmids, sorted into a shMID1-GFP$^+$ and an shMID1-GFP$^-$ subpopulation, and stimulated for 4 h with $gp_{33–41}$ pulsed splenocytes. The supernatants were harvested and the concentration of secreted granzyme B and IFN-γ determined. Secretion of granzyme B was reduced by approximately 70% in shMID1-GFP$^+$ P14 CTLs compared with shMID1-GFP$^-$ P14 CTLs, whereas IFN-γ secretion was unaffected by MID1 knockdown (Fig. 5D and E). QPCR analyses demonstrated that MID1 expression was reduced by approximately 50% in shMID1-GFP$^+$ P14 CTLs compared with shMID1-GFP$^-$ P14 CTLs (Fig. 5F). Taken together, these results show that MID1 controls exocytosis of lytic granules in CTLs.

Discussion

In this study, we show that MID1 controls exocytosis of lytic granules and cytotoxicity in CTL. MID1 is a microtubule-associated ubiquitin ligase that regulates the level of microtubule-associated PP2Ac in embryonic fibroblasts [12–15]. MID1 is causally linked to OS and plays important roles in the formation of diverse ventral midline structures during embryogenesis [16]. Whether MID1 is expressed in T cells or plays any biological role in these was not known until the present study.

We found that *MID1* mRNA is weakly expressed in murine thymocytes and naïve T cells. This is in good agreement with

previous studies, which found that although *MID1* is widely expressed during embryogenesis, it is mainly found in the brain, heart, kidney, lung, and placenta and only weakly expressed in thymus and spleen in adult tissues [16, 20, 21]. The low expression of *MID1* in thymocytes also concurs with our observation that T-cell development is not affected in P14MID1$^{-/-}$ mice. Likewise, the weak *MID1* expression in naïve T cells might also explain why activation and expansion of naïve P14MID1$^{-/-}$ T cells were unaffected. We show that *MID1* becomes significantly upregulated following activation and differentiation of mouse CD8$^+$ T cells. The activation-induced upregulation of *MID1* was specific for CD8$^+$ T cells and was not seen in CD4$^+$ T cells. Differential gene expression in activated CD4$^+$ and CD8$^+$ T cells, as observed for *MID1* in this study, is not exceptional but has been reported for several genes including *Prf1* (perforin) and *Gzmb* (granzyme B) [30].

Recently, it has been described that fibroblasts derived from OS patients harboring a mutated *MID1* have defects in mTORC1 function as measured by impaired phosphorylation of S6K1 [27]. In parallel, it was found that knockdown of MID1 in the human osteosarcoma cell line U2OS reduced mTORC1 function and S6K1 phosphorylation. In accordance, we found that MID1 affected TCR signaling, and that S6K1 phosphorylation was strongly impaired in P14MID1$^{-/-}$ CTLs. Activation of ERK1/2 was also impaired in P14MID1$^{-/-}$ CTLs, whereas proximal TCR signaling as determined by ZAP70 phosphorylation was unaffected. PP2A plays a major role in down regulation of ERK1/2 activity [31] and our results strongly indicate that the PP2A activity in P14MID1$^{-/-}$ CTLs is increased as previously observed in fibroblasts from OS patients [14]. This was further supported by the increased levels of PP2Ac in stimulated P14MID1$^{-/-}$ CTLs. The reverse scenario where MID1 upregulation leads to PP2A downregulation has recently been described in relation to airway inflammation [18] and Huntington's disease [32]. Whether the impaired mTORC1 function we observed as reduced S6K1 phosphorylation in P14MID1$^{-/-}$ CTLs is caused by a direct inhibitory effect of PP2A on mTORC1, as suggested for MID1-deficient cell lines [27], or indirectly via increased TSC2 activity caused by the reduced ERK1/2 activity [33] or by other mechanisms requires further studies to be determined. The molecular mechanisms that drive MTOC polarization are poorly understood; however, several molecules in the TCR signaling pathways including ERK1/2 [8, 34] have been implicated in MTOC polarization to the IS. In accordance with the affected TCR signaling and reduced ERK1/2 activation, we found that polarization of the MTOC was impaired in P14MID1$^{-/-}$ CTLs. In line with this, shRNA-mediated knockdown of MID1 in P14 CTLs reduced MTOC polarization, and furthermore we could rescue MTOC polarization in P14MID1$^{-/-}$ CTLs by inserting MID1. In contrast to the MTOC polarization defects, the overall microtubules network seemed normal. This is in agreement with reports describing the role of MID1 in fibroblasts from Opitz patients [13] and embryonic fibroblasts from MID1$^{-/-}$ mice (GM, personal communication).

The capacity of P14MID1$^{-/-}$ CTLs to kill target cells was impaired and this correlated with reduced exocytosis of lytic granules from P14MID1$^{-/-}$ CTLs. Agents that depolymerize microtubules inhibit target cell killing [5, 28], which underlines the central role of stable microtubules in trafficking of the lytic granules to the IS [6]. Interestingly, it has been suggested that MID1 stabilizes the microtubules during embryogenesis [13], and we propose that one mechanism by which MID1 regulates exocytosis of lytic granules is by stabilizing the microtubules in CTLs. This is further supported by the observation that overexpression of MID1 increased exocytosis of lytic granules by approximately 100% even in P14 CTLs. In contrast to the impaired exocytosis of lytic granules, we found that secretion of IFN-γ and TNF-α was unaffected in P14MID1$^{-/-}$ CTLs and by overexpression of MID1. This indicates that these cytokines use a different MID1-independent secretory pathway than lytic granules, which is in good agreement with previous studies describing the existence of different secretory pathways for lytic granules and cytokines in T cells [8, 35]. Interestingly, whereas overexpression of MID1 significantly increased exocytosis of lytic granules, it did not affect MTOC polarization in P14 CTLs. This suggests that different MID1-mediated mechanisms regulate exocytosis of lytic granules and polarization of the MTOC, and that these processes can take place independently of each other as recently suggested [36].

It is intriguing to speculate that OS patients might have a compromised CTL response, but very little has been published on this matter. Most clinical reports describe the developmental anatomical defects, which are the main features of the disorder. Further, OS is diagnosed at birth or in the first years of age, but are rarely followed up. Cases of pneumonia have been reported but they are usually attributed to aspiration/respiratory distress probably secondary to trachea-esophageal abnormalities (personal communications to GM).

In conclusion, our data show that MID1 is expressed in CTLs where it controls TCR signaling, MTOC organization, and release of cytolytic mediators. Thus, MID1 orchestrates multiple events in CTL responses adding a novel level of regulation of CTL activation and cytotoxicity. In addition to providing significant knowledge on MID1 protein function in CTL biology, our study may well have implications for regulated granule exocytosis in other cell types such as pancreatic β-cells, natural killer cells, and mast cells, as many of the same molecules are involved in granule exocytosis in these cells [37, 38].

Materials and methods

Mice and cell lines

Generation of the MID1$^{-/-}$ mouse strain has been described [39]. The P14 mice (transgenic line 318) express the transgenic Vα2Vβ8 TCR specific for the LCMV glycoprotein $gp_{33–41}$ when bound to H-2D^b [40, 41], and SMARTA mice express the transgenic Vα2Vβ8 TCR specific for the LCMV glycoprotein $gp_{61–80}$ when bound to I-A^b [42]. The MID1$^{-/-}$, P14, and SMARTA strains were all on

a C57BL/6 background. MID1$^{-/-}$ mice were crossed to P14 mice to generate P14MID1$^{-/-}$ mice. Splenocytes from C57BL/6 mice were used as APC. Animal experiments were approved by the Animal Experiments Inspectorate, The Danish Ministry of Justice (approval number 2007/561–1357). EL-4 cells were cultured in complete medium (RPMI 1640 supplemented with 10% FBS, 1% L-glutamine, 0.5 IU/L penicillin, 500 mg/L streptomycin, and 50 μM 2-ME) at 37°C in 5% CO_2.

Expansion of T cells and FACS analysis

Murine P14 and P14MID1$^{-/-}$ CTLs were generated by stimulating splenocytes isolated from TCR transgenic P14 and P14MID1$^{-/-}$ female mice with 5 ng/mL of LCMV gp_{33-41} (Schafer-N) for 3 days in complete medium and subsequently resting them for 2 days as previously described [43]. For murine FACS analyses of cell surface and intracellular molecules, we used antibodies against CD8 (53–6.7), TCRVβ8 (F23.1), TCRVα2 (B20.1), CD62L (MEL-14), CD44 (IM7), IFN-γ (XMG1.2), and TNF-α (MP6.XT22) all from BD Biosciences, granzyme B (GB11, Invitrogen) and perforin (eBioOMAK-D, eBioscience). For phenotyping, cells from thymus, spleen, and LNs were isolated, stained with antibodies against CD4 (RM4–5), CD8 (53–6.7), TCRVα2 (B20.1), and CD19 (1D3) from BD Biosciences, and analyzed by FACS as previously described [44]. For CD107a staining CTLs were restimulated for the time indicated with 100 ng/mL gp_{33-41} in the presence of CD107a-FITC antibody (1D4B from BD Biosciences) and 3 μM monensin as previously described [29]. After incubation, the cells were surface stained with antibodies against CD8, Vα2, and CD44 as described above.

Quantitative PCR analysis

Total RNA was extracted from thymocytes, purified naïve CD4$^+$ and CD8$^+$ T cells, activated CD4$^+$ T cells, and CTLs using Trizol. One microgram of total RNA from each sample was reverse-transcribed into cDNA using RevertAid First Strand cDNA Synthesis Kit (Fermentas). *MID1* and β-*actin* gene expression was determined using primers from TAG-Copenhagen and Stratagene Brilliant SYBR® Green QPCR Master Mix (Agilent Technologies). Murine *MID1* gene expression was calculated relative to β-*actin* gene. Results were normalized to control conditions using the $2^{-\Delta\Delta Ct}$ method [45]. Primers were MID1-forward 5′ GCT CCC AGT AAA GAC AGA C 3′, MID1-reverse 5′ GAG CCC GTC TAG ACC TCGC 3′, β-actin-forward 5′ AAG TGT GAC GTT GAC ATC 3′, β-actin-reverse 5′ TGC CTG GGT ACA TGG TGG 3′.

CTL-target cell conjugation and cytotoxicity assays

For CTL-target cell conjugations assays, EL-4 cells were preincubated with 0.1 μM CFSE (Invitrogen) and pulsed for 1 h with 0 or 100 ng/mL gp_{33-41}. EL-4 cells and CTLs were mixed at a 1:1 ratio, spun down for 5 s and incubated for 15 min at 37°C. The cells were then fixed for 10 min at 37°C with an equal volume of 4% paraformaldehyde. The cells were washed and stained with antibodies against CD8 and analyzed by FACS. The fraction of CTLs that formed stable conjugates with the target cells were calculates as (CD8$^+$CFSE$^+$ events/total CD8$^+$ events) × 100%. For FACS-based cytotoxicity assays, EL-4 cells were pulsed with 0 or 100 ng/mL gp_{33-41} and used as target cells. CTLs and EL-4 cells were mixed in 96-well round-bottomed plates at the indicated effector to target cell ratios, spun down for 5 s and co-cultured for the time indicated. The cells were then stained with antibodies against CD8 and Annexin V and propidium iodide (PI) from BD Biosciences and analyzed by FACS. The fraction of CD8$^-$ cells that stained positive for Annexin V and/or PI was recorded as dead target cells.

Granzyme B, IFN-γ, and TNF-α secretion

CTLs and splenocytes prepulsed with 100 ng/mL gp_{33-41} were mixed, spun down for 5 s, and co-cultured for 4 h as previously described [43]. The supernatants were harvested and the concentration of granzyme B, IFN-γ, and TNF-α was subsequently measured by ELISA as described by the supplier (eBioscience).

MID1-GFP transfection and RNA interference

For MID1 overexpression studies, 5 × 10^6 P14 and P14MID1$^{-/-}$ CTLs were resuspended in 100 μL of Amexa Mouse T cell Nucleofector kit, mixed with MID1-GFP (a gift from Susann Schweiger [13]) or control-GFP (KM28212G, SABiosciences) plasmids, and transfected using program X-01 on the Amexa Nucleofector I system. The cells were rested for 4 h at 37°C and subsequently sorted on a FACS-Aria II (BD Biosciences) in an MID1-GFP$^+$ and an MID1-GFP$^-$ subpopulation for MID1 transfections and in a control-GFP$^+$ and a control-GFP$^-$ subpopulation for control-GFP transfections. The GFP$^+$ and GFP$^-$ CTLs were co-cultured with splenocytes that had been pulsed with 100 ng/mL gp_{33-41}. The cells were incubated for 4 h, and the supernatants were subsequently analyzed for granzyme B, IFN-γ and TNF-α by ELISA. For MID1 RNA interference, 5 × 10^6 P14 and P14MID1$^{-/-}$ CTLs were resuspended in 100 μL of Amexa Mouse T-cell Nucleofector kit, mixed with a total of 4 μg SureSilencing shRNA-MID1-GFP plasmids 1–4 (KM28212G, SABiosciences), and immediately transfected using program X-01 on the Amexa Nucleofector I system. The cells were rested for 24 h at 37°C and subsequently sorted on a FACS-Aria II into shMID1-GFP$^+$ and shMID1-GFP$^-$ subpopulations. The shMID1-GFP$^+$ and shMID1-GFP$^-$ CTLs were added to splenocytes that had been pulsed with 100 ng/mL gp_{33-41}. The cells were incubated for 4 h, and the supernatants were subsequently analyzed for granzyme B and IFN-γ by ELISA.

Western blots

CTLs were stimulated for 0–6 h with 100 ng/mL gp_{33-41}. Total PP2Ac, c-Cbl, ERK1/2, S6K1, and GAPDH and phosphorylated ZAP70, ERK1/2, and S6K1 were determined by

western blots as previously described [46, 47] using anti-PP2Ac (52F8, Cell Signaling), anti-c-Cbl (7G10, Upstate Biotechnology), anti-ERK1/2 (#9102, Cell Signaling), anti-S6K1 (49D7, Cell Signaling), anti-GAPDH (ab9485, Abcam), anti-pZAP70 Tyr319 (#2701), anti-pERK1/2 Thr202/Tyr204 (#9101), and anti-pS6K1 Thr421/Ser424 (#9204) all from Cell Signaling. Semiquantification was done using Fiji software and the density calculated as (normalized band density$_{t=x}$ /normalized band density$_{t=0}$) $\times$ 100%. PP2Ac was normalized to c-Cbl. pZAP70, pERK1/2 and pS6K1 to GAPDH.

MTOC polarization

CTLs were resuspended in PBS supplemented with 50 nM TubulinTracker green (Invitrogen) and plated on coverslips coated with poly-L-lysine and anti-CD3 antibodies (145-2C11, BD Biosciences). The cells were kept at 37°C and z-stacks were acquired using a Zeiss Cell Observer with spinning disc and a 100×/1.46 NA oil objective. The z-stacks were blinded, the absolute position of the MTOC found and scored from 0 to 1 relative to the cell size. A low number indicates MTOC polarization toward the coverslip, whereas a high number indicates MTOC positioning away from the coverslip as depicted in Figure 3E.

Statistical analysis

Statistical analyses were performed using Student's *t*-test with a 5% significance level, unpaired observations, and equal variance. MTOC statistical analyses were performed using Mann–Whitney nonparametric test.

Acknowledgments: The expert technical help of Bodil Nielsen is gratefully acknowledged. We would also like to acknowledge The Cluster in Biomedicine, AREA Science Park, Trieste, Italy. L.B. and C.G. was supported by The Danish Medical Research Council. C.G. was also supported by The Novo Nordisk Foundation, The Lundbeck Foundation, and The A.P. Møller Foundation for the Advancement of Medical Sciences.

L.B. and A.K.H. did most of the experiments, analyzed data, and contributed to the writing of the manuscript. B.B.J. and T.H.B. contributed to the MTOC experiments. M.R.v.E., N.Ø., G.M., C.M.B., M.K., B.A.H.J., A.R.T., and A.W. contributed to the planning, designing, and analyses of some of the experiments, and writing of the manuscript. C.G. conceptualized the research, directed the study, analyzed data, and wrote the manuscript.

Conflict of interest: The authors declare no commercial or financial conflict of interest.

References

1 **Monks, C. R., Freiberg, B. A., Kupfer, H., Sciaky, N. and Kupfer, A.**, Three-dimensional segregation of supramolecular activation clusters in T cells. *Nature* 1998. **395**: 82–86.

2 **Grakoui, A., Bromley, S. K., Sumen, C., Davis, M. M., Shaw, A. S., Allen, P. M. and Dustin, M. L.**, The immunological synapse: a molecular machine controlling T cell activation. *Science* 1999. **285**: 221–227.

3 **Stinchcombe, J. C., Bossi, G., Booth, S. and Griffiths, G. M.**, The immunological synapse of CTL contains a secretory domain and membrane bridges. *Immunity* 2001. **15**: 751–761.

4 **Geiger, B., Rosen, D. and Berke, G.**, Spatial relationships of microtubule-organizing centers and the contact area of cytotoxic T lymphocytes and target cells. *J. Cell Biol.* 1982. **95**: 137–143.

5 **Kupfer, A. and Dennert, G.**, Reorientation of the microtubule-organizing center and the Golgi apparatus in cloned cytotoxic lymphocytes triggered by binding to lysable target cells. *J. Immunol.* 1984. **133**: 2762–2766.

6 **Stinchcombe, J. C., Majorovits, E., Bossi, G., Fuller, S. and Griffiths, G. M.**, Centrosome polarization delivers secretory granules to the immunological synapse. *Nature* 2006. **443**: 462–465.

7 **Stinchcombe, J. C. and Griffiths, G. M.**, Secretory mechanisms in cell-mediated cytotoxicity. *Annu. Rev. Cell Dev. Biol.* 2007. **23**: 495–517.

8 **Huse, M., Quann, E. J. and Davis, M. M.**, Shouts, whispers and the kiss of death: directional secretion in T cells. *Nat. Immunol.* 2008. **9**: 1105–1111.

9 **Trapani, J. A. and Smyth, M. J.**, Functional significance of the perforin/granzyme cell death pathway. *Nat. Rev. Immunol.* 2002. **2**: 735–747.

10 **Schweiger, S. and Schneider, R.**, The MID1/PP2A complex: a key to the pathogenesis of Opitz BBB/G syndrome. *Bioessays* 2003. **25**: 356–366.

11 **Meroni, G. and Diez-Roux, G.**, TRIM/RBCC, a novel class of 'single protein RING finger' E3 ubiquitin ligases. *Bioessays* 2005. **27**: 1147–1157.

12 **Cainarca, S., Messali, S., Ballabio, A. and Meroni, G.**, Functional characterization of the Opitz syndrome gene product (midin): evidence for homodimerization and association with microtubules throughout the cell cycle. *Hum. Mol. Genet.* 1999. **8**: 1387–1396.

13 **Schweiger, S., Foerster, J., Lehmann, T., Suckow, V., Muller, Y. A., Walter, G., Davies, T. et al.**, The Opitz syndrome gene product, MID1, associates with microtubules. *Proc. Natl. Acad. Sci. USA* 1999. **96**: 2794–2799.

14 **Trockenbacher, A., Suckow, V., Foerster, J., Winter, J., Krauss, S., Ropers, H. H., Schneider, R. et al.**, MID1, mutated in Opitz syndrome, encodes an ubiquitin ligase that targets phosphatase 2A for degradation. *Nat. Genet.* 2001. **29**: 287–294.

15 **Liu, J., Prickett, T. D., Elliott, E., Meroni, G. and Brautigan, D. L.**, Phosphorylation and microtubule association of the Opitz syndrome protein mid-1 is regulated by protein phosphatase 2A via binding to the regulatory subunit alpha 4. *Proc. Natl. Acad. Sci. USA* 2001. **98**: 6650–6655.

16 **Quaderi, N. A., Schweiger, S., Gaudenz, K., Franco, B., Rugarli, E. I., Berger, W., Feldman, G. J. et al.**, Opitz G/BBB syndrome, a defect of midline development, is due to mutations in a new RING finger gene on Xp22. *Nat. Genet.* 1997. **17**: 285–291.

17 **De Falco, F., Cainarca, S., Andolfi, G., Ferrentino, R., Berti, C., Rodriguez, C. G., Rittinger, O. et al.**, X-linked Opitz syndrome: novel mutations in the MID1 gene and redefinition of the clinical spectrum. *Am. J. Med. Genet. A* 2003. **120A**: 222–228.

18 **Collison, A., Hatchwell, L., Verrills, N., Wark, P. A., de Siqueira, A. P., Tooze, M., Carpenter, H. et al.**, The E3 ubiquitin ligase midline 1 promotes allergen and rhinovirus-induced asthma by inhibiting protein phosphatase 2A activity. *Nat. Med.* 2013. **19**: 232–237.

19 **Dal Zotto, L., Quaderi, N. A., Elliott, R., Lingerfelter, P. A., Carrel, L., Valsecchi, V., Montini, E. et al.**, The mouse Mid1 gene: implications for the pathogenesis of Opitz syndrome and the evolution of the mammalian pseudoautosomal region. *Hum. Mol. Genet.* 1998. **7**: 489–499.

20 **Van den Veyver, I. B., Cormier, T. A., Jurecic, V., Baldini, A. and Zoghbi, H. Y.**, Characterization and physical mapping in human and mouse of a novel RING finger gene in Xp22. *Genomics* 1998. **51**: 251–261.

21 **Landry, J. R. and Mager, D. L.**, Widely spaced alternative promoters, conserved between human and rodent, control expression of the Opitz syndrome gene MID1. *Genomics* 2002. **80**: 499–508.

22 **Janssens, V. and Goris, J.**, Protein phosphatase 2A: a highly regulated family of serine/threonine phosphatases implicated in cell growth and signalling. *Biochem. J.* 2001. **353**: 417–439.

23 **Shi, Y.**, Serine/threonine phosphatases: mechanism through structure. *Cell* 2009. **139**: 468–484.

24 **Junttila, M. R., Li, S. P. and Westermarck, J.**, Phosphatase-mediated crosstalk between MAPK signaling pathways in the regulation of cell survival. *FASEB J.* 2008. **22**: 954–965.

25 **Cantrell, D.**, T cell antigen receptor signal transduction pathways. *Annu. Rev. Immunol.* 1996. **14**: 259–274.

26 **Tsun, A., Qureshi, I., Stinchcombe, J. C., Jenkins, M. R., de la Roche, M., Kleczkowska, J., Zamoyska, R. et al.**, Centrosome docking at the immunological synapse is controlled by Lck signaling. *J. Cell Biol.* 2011. **192**: 663–674.

27 **Liu, E., Knutzen, C. A., Krauss, S., Schweiger, S. and Chiang, G. G.**, Control of mTORC1 signaling by the Opitz syndrome protein MID1. *Proc. Natl. Acad. Sci. USA* 2011. **108**: 8680–8685.

28 **Katz, P., Zaytoun, A. M. and Lee, J. H., Jr.**, Mechanisms of human cell-mediated cytotoxicity. III. Dependence of natural killing on microtubule and microfilament integrity. *J. Immunol.* 1982. **129**: 2816–2825.

29 **Betts, M. R., Brenchley, J. M., Price, D. A., De Rosa, S. C., Douek, D. C., Roederer, M. and Koup, R. A.**, Sensitive and viable identification of antigen-specific CD8+ T cells by a flow cytometric assay for degranulation. *J. Immunol. Methods* 2003. **281**: 65–78.

30 **Weng, N. P., Araki, Y. and Subedi, K.**, The molecular basis of the memory T cell response: differential gene expression and its epigenetic regulation. *Nat. Rev. Immunol.* 2012. **12**: 306–315.

31 **Millward, T. A., Zolnierowicz, S. and Hemmings, B. A.**, Regulation of protein kinase cascades by protein phosphatase 2A. *Trends Biochem. Sci.* 1999. **24**: 186–191.

32 **Krauss, S., Griesche, N., Jastrzebska, E., Chen, C., Rutschow, D., Achmuller, C., Dorn, S. et al.**, Translation of HTT mRNA with expanded CAG repeats is regulated by the MID1-PP2A protein complex. *Nat. Commun.* 2013. **4**: 1511.

33 **Zoncu, R., Efeyan, A. and Sabatini, D. M.**, mTOR: from growth signal integration to cancer, diabetes and ageing. *Nat. Rev. Mol. Cell Biol.* 2011. **12**: 21–35.

34 **Chen, X., Allan, D. S., Krzewski, K., Ge, B., Kopcow, H. and Strominger, J. L.**, CD28-stimulated ERK2 phosphorylation is required for polarization of the microtubule organizing center and granules in YTS NK cells. *Proc. Natl. Acad. Sci. USA* 2006. **103**: 10346–10351.

35 **Huse, M., Lillemeier, B. F., Kuhns, M. S., Chen, D. S. and Davis, M. M.**, T cells use two directionally distinct pathways for cytokine secretion. *Nat. Immunol.* 2006. **7**: 247–255.

36 **Bertrand, F., Muller, S., Roh, K. H., Laurent, C., Dupre, L. and Valitutti, S.**, An initial and rapid step of lytic granule secretion precedes microtubule organizing center polarization at the cytotoxic T lymphocyte/target cell synapse. *Proc. Natl. Acad. Sci. USA* 2013. **110**: 6073–6078.

37 **Hou, J. C., Min, L. and Pessin, J. E.**, Insulin granule biogenesis, trafficking and exocytosis. *Vitam. Horm.* 2009. **80**: 473–506.

38 **Metz, M. and Maurer, M.**, Mast cells–key effector cells in immune responses. *Trends Immunol.* 2007. **28**: 234–241.

39 **Lancioni, A., Pizzo, M., Fontanella, B., Ferrentino, R., Napolitano, L. M., De, L. E. and Meroni, G.**, Lack of mid1, the mouse ortholog of the opitz syndrome gene, causes abnormal development of the anterior cerebellar vermis. *J. Neurosci.* 2010. **30**: 2880–2887.

40 **Pircher, H., Moskophidis, D., Rohrer, U., Burki, K., Hengartner, H. and Zinkernagel, R. M.**, Viral escape by selection of cytotoxic T cell-resistant virus variants in vivo. *Nature* 1990. **346**: 629–633.

41 **Bonefeld, C. M., Haks, M., Nielsen, B., Von, E. M., Boding, L., Hansen, A. K., Larsen, J. M. et al.**, TCR down-regulation controls virus-specific $CD8^+$ T cell responses. *J. Immunol.* 2008. **181**: 7786–7799.

42 **Oxenius, A., Bachmann, M. F., Zinkernagel, R. M. and Hengartner, H.**, Virus-specific MHC-class II-restricted TCR-transgenic mice: effects on humoral and cellular immune responses after viral infection. *Eur. J. Immunol.* 1998. **28**: 390–400.

43 **Hansen, A. K., Regner, M., Bonefeld, C. M., Boding, L., Kongsbak, M., Odum, N., Mullbacher, A. et al.**, TCR down-regulation boosts T-cell-mediated cytotoxicity and protection against poxvirus infections. *Eur. J. Immunol.* 2011. **41**: 1948–1957.

44 **Boding, L., Bonefeld, C. M., Nielsen, B. L., Lauritsen, J. P., von Essen, M. R., Hansen, A. K., Larsen, J. M. et al.**, TCR down-regulation controls T cell homeostasis. *J. Immunol.* 2009. **183**: 4994–5005.

45 **Livak, K. J. and Schmittgen, T. D.**, Analysis of relative gene expression data using real-time quantitative PCR and the $2^{-\Delta\Delta Ct}$ method. *Methods* 2001. **25**: 402–408.

46 **Nielsen, M., Svejgaard, A., Skov, S., Dobson, P., Bendtzen, K., Geisler, C. and Odum, N.**, IL-2 induces beta2-integrin adhesion via a wortmannin/LY294002-sensitive, rapamycin-resistant pathway. Phosphorylation of a 125-kilodalton protein correlates with induction of adhesion, but not mitogenesis. *J. Immunol.* 1996. **157**: 5350–5358.

47 **Dietrich, J. and Geisler, C.**, T cell receptor zeta allows stable expression of receptors containing the CD3γ leucine-based receptor-sorting motif. *J. Biol. Chem.* 1998. **273**: 26281–26284.

Abbreviations: **CTL**: cytotoxic lymphocyte · **IS**: immunological synapse · **LCMV**: lymphocytic choriomeningitis virus · **MID1**: midline 1 · **MTOC**: microtubule-organizing center · **OS**: X-linked Opitz G/BBB syndrome · **PI**: propidium iodide · **PP2A**: protein phosphatase 2A

Full correspondence: Dr. Carsten Geisler, Department of International Health, Immunology and Microbiology, Faculty of Health and Medical Sciences, Blegdamsvej 3, University of Copenhagen, DK-2200 Copenhagen, Denmark
Fax: +45-3532-7853
e-mail: cge@sund.ku.dk

Received: 13/12/2013
Revised: 27/5/2014
Accepted: 8/7/2014
Accepted article online: 12/7/2014

